

Further variability of the compact radio nebula of P Cygni

K. M. Exter,¹★ S. K. Watson,² M. J. Barlow³ and R. J. Davis²

¹*APS Division, Department of Pure & Applied Physics, Queen's University Belfast, Belfast BT7 1NN*

²*University of Manchester, Jodrell Bank Observatory, Macclesfield, Cheshire SK11 9DL*

³*University College London, Gower Street, London WC1E 6BT*

Accepted 2002 February 27. Received 2002 January 11; in original form 2001 February 15

ABSTRACT

Skinner et al. presented two high-resolution 6-cm (5 GHz) images of the B-supergiant star P Cygni. These show the observed morphology and flux densities to have changed over the intervening month. Following on from this, we present a series of seven high-resolution 6-cm images (including re-reductions of the two from Skinner et al.). These confirm that radio emission from the inner 400 mas of the wind is inhomogeneous, consisting usually of several separated bright spots, and that the total and peak flux densities and the observed morphology vary over all time-scales sampled. We suggest that recombination in cooling clumps of gas which will decrease the radio emission, followed by the appearance of other ionized clumps, could explain such rapid changes, but detailed models must await further observations.

Key words: stars: imaging – stars: individual: P Cygni – supergiants – radio continuum: stars.

1 INTRODUCTION

P Cygni is of the class of S Dor (or luminous blue) variable stars, which are massive stars situated in an unstable part of the Hertzsprung–Russell diagram (for a recent review see Israelian & de Groot 1999). It was the first early-type single star from which radio emission was detected, by Wendker, Baars & Altenhoff (1973), and it has been observed sporadically ever since then. Observations show emission from the wind (as an unresolved point source in most images, first identified by White & Becker 1992) with additional emission extended out to possibly beyond 1 arcmin (Baars & Wendker 1987; Scuderi et al. 1998).

The deepest radio observations, published by Skinner et al. (1998), were the sum of seven years of 2- and 6-cm Very Large Array (VLA) monitoring. The morphologies at the two wavelengths are similar; the inner few hundred milliarcsec (mas) region is unresolved, and it is surrounded by a filamentary or blobby nebula over a slightly asymmetric region of ~ 20 arcsec diameter, with fainter emission extending to almost an arcminute from the star. These data, along with additional 6-cm monthly monitoring, also produced radio light curves that show the flux density to vary by about ± 10 per cent about the mean values of 10 mJy at 6 cm and 17 mJy at 2 cm. The time-scales are as little as a few days, and changes of 20–50 per cent are not infrequently observed.

The highest resolution radio images of P Cygni were reported by Skinner et al. (1997). Two observations were taken with the Multi-Element Radio Linked Interferometer Network (MERLIN) at 6 cm spaced by a month, with a resolution of 50 mas. These images show

emission only within the inner 400 mas around the map centre, consisting of a few separated 50-mas-sized peaks, which changed in position and flux density over the intervening month. Following on from this study, we decided to use MERLIN to map P Cygni at 6 cm over a series of time-scales, in order to see what the shortest time-scale of the variations may be. The results of this study are reported here.

2 THE OBSERVATIONS

Nine sets of data (in 1992, 1997 and 2001) were taken at 6 cm with MERLIN, using six telescopes, those at Cambridge, Knockin, Defford, Darnhall and Tabley, and the Mark II telescope at Jodrell Bank. The two 1992 data sets recorded here as observed on 1992 July 1 and 1992 August 4 are the same as the MERLIN data sets of Skinner et al. (1997), which were misidentified as being observed on 1992 August 4 and 1992 June 24 respectively. After 1992, MERLIN was significantly upgraded and new data reduction tasks written. In order for reliable comparison to be made between the 1992 and later data, we have (re-)reduced the former along with the latter. For all epochs both right- and left-hand circular polarizations were recorded with a bandwidth of 15 MHz. The observations were made in phase-referencing mode, spending ~ 4 min (~ 7 min in 1992) on the target source and switching regularly to the phase calibrator 2007+405 for ~ 2 min. Two of the 1997 data sets proved unusable because of insufficient signal-to-noise ratio and we provide no map of these, although the total flux density for one (1997 January 16) is given. The data of 1992 August 4 have higher errors than the rest because of greater uncertainty in the flux calibration source data. Details of the observations are given in Table 1.

★E-mail: k.exter@qub.ac.uk

Table 1. Observation dates, frequencies, on-source integration times on P Cygni, and the name of and flux density measured for the point calibration sources, and the derived flux density of the phase calibrator (2007+405).

Date	ν_0 (GHz)	t_{int} (min)	Point source name	S_ν (Jy)	Phase cal. S_ν (Jy)
1992 July 1	4.993	776	0552+398	7.09	3.47
1992 August 4	4.993	748	0552+398	7.02	3.64
1997 January 15	4.994	382	OQ208	3.24	4.16
1997 January 16	4.994	403	0234+285	2.46	4.19
1997 January 19	4.994	785	0234+285	2.44	4.04
1997 January 30	4.994	680	0552+398	5.79	3.66
1997 February 27	4.994	638	0552+398	5.76	2.80
2001 May 8	4.994	1075	OQ208	2.09	2.30

The flux calibration was carried out using the unresolved sources 0552+398, 0234+285 and OQ 208, which were themselves calibrated against 3C 286, using the flux density scale of Baars et al. (1977). Initial calibration was carried out using the MERLIN-specific software procedure DPROC, with which the absolute flux scale for the observations was determined. Subsequent calibration and mapping were carried out using the AIPS package.

The phase calibrator 2007+405 was mapped with three passes of self-calibration over a 512×512 pixel field, and was found to be a point source at any contour above ~ 0.3 per cent of the maximum flux density. The data were then re-weighted to take into account the differing telescope sensitivities. As P Cygni is a relatively weak radio source, the derived antenna gain solutions from the phase calibrator were interpolated to calibrate the data for P Cygni. The right- and left-hand polarization data for the target were then added and the frequency channels were averaged into a single channel.

The images were made using a pixel size of 15 mas, which resulted in a final CLEANed field of size 7.68×7.68 arcsec², initially using a field of about ~ 200 mas diameter centred on the source, and then over the entire field. The data were weighted midway between uniform and natural weighting (robust = 1), thereby optimizing both the rms noise levels and the resolution of the images. The data were mapped with a half-power beamwidth of 50 mas in both directions. The uv coverages for all the observations were similar to each other.

We re-reduced the two 1992 images previously shown in Skinner et al. (1997). The primary difference is that this time we did not self-calibrate P Cygni (its rather low flux density does not encourage the self-calibration procedure), used a new weighting procedure, and used a different method to measure the total flux densities. The structural appearance and relative flux density levels are insignificantly affected by these changes, but the absolute flux density values have almost doubled.

3 RESULTS

Fig. 1 shows maps of all the epochs of data. Note that the proper motion was not accounted for when creating these maps (see later, however). Of the area CLEANed, only in the portion shown in the maps is there any significant flux above the noise. In these images we see significant variations to both the structure and the flux

density (S_ν) levels. In Table 2 are listed the total flux density per beam and the brightest peak flux density per beam for all data sets, and Table 3 further lists the flux densities and positions of the brightest peaks on the sequence of January maps. The errors are an average of the rms value measured from regions far from the central source. The total flux density values were measured by summing the flux within a box placed around the regions of emission of $\geq 3\sigma$ for each date (which can be seen from Fig. 1). These are provided for comparison only between the sequences of images presented here. Observations made with arrays with shorter baselines (e.g. the VLA) will be sensitive to emission on larger spatial scales (and vice versa), and will therefore measure different values of flux density, and different data reduction methods also affect the value of flux density recorded. The peak brightness temperatures (T_b) in Table 2 are calculated from Krauss (1966):

$$T_b = \frac{S_\nu \lambda^2}{2k\Omega},$$

where Ω is the solid angle over which the calculation is made (in this case, the beamsize). The brightness temperature is the blackbody temperature for a source of that flux density over that area.

Figs 2 and 3 are overlays of the maps of 1997 January 15 with January 19 and January 19 with January 30, respectively. The lowest contour/grey-scale is 3σ , where σ is the average error for all three maps ($0.133 \text{ mJy beam}^{-1}$), and the highest contour/grey-scale matches the peak values quoted in Table 2. From these it can clearly be seen that the morphology has changed between each set of dates (and, although not shown, over the other dates also), in that the positions of the brightest peaks have changed. The entries of Tables 2 and 3 show that the peak and total flux densities vary between the observed dates, with the mean and standard deviation over all dates being $8.17 \pm 2.30 \text{ mJy}$ (28 per cent) total and $0.95 \pm 0.44 \text{ mJy beam}^{-1}$ (46 per cent) peak.

The Carlsberg Automatic Meridian Telescope measured the optical position and the proper motion (-0.6 ms yr^{-1} in RA, -5 mas yr^{-1} in declination) for P Cygni in 1991.18. Correcting for the proper motion and differences in equinox with the MERLIN observations (FK4 for the radio, FK5 for the optical), we have derived epoch 1950, equinox 1950 positions for the centre of symmetry of the radio images of 1997 February and 1992 August, and for the 1991.18 optical position, which agree to within their respective errors (given in brackets as the last significant digit). The positions are RA(1950) $20^{\text{h}} 15^{\text{m}}+$ and Dec. (1950) $37^{\circ}52'+$

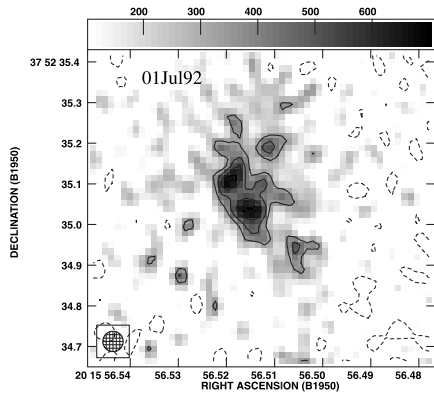
optical(1991.18): $56:542(4)$, $35:31(5)$;
radio(1992.58): $56:541(6)$, $35:26(1)$;
radio(1997.16): $56:542(6)$, $35:26(1)$.

Thus the radio emission is indeed situated around the star.

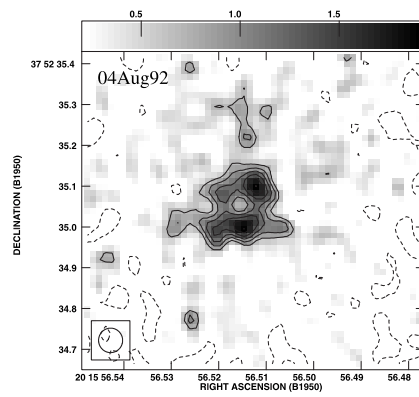
4 TESTING THE MAPS

Although the integrated 6-cm flux density of P Cygni is among the brightest found for a thermal wind source, the very high angular resolution of MERLIN means that the observed features are not of very high signal-to-noise ratio.

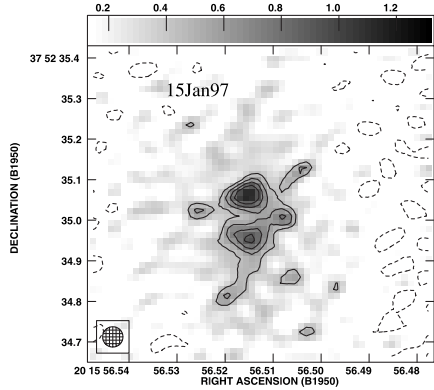
Figure 1. 6-cm MERLIN image of P Cygni taken at the different epochs, as labelled. Contours are $-1, 3, 4, 5, 6$ times the rms noise (up to 7 for the 1992 August map). The grey-scale starts at 1 times the rms noise and scales up to the peak flux density per beam. The beam, plotted in the corner, is 50 mas in diameter, and sets the resolution.



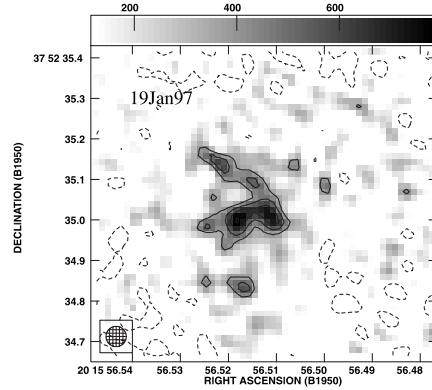
rms noise = 0.11 mJy/bm
peak flux = 0.76 mJy/bm



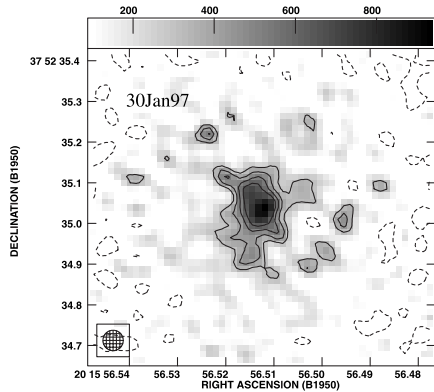
rms noise = 0.23 mJy/bm
peak flux = 1.80 mJy/bm



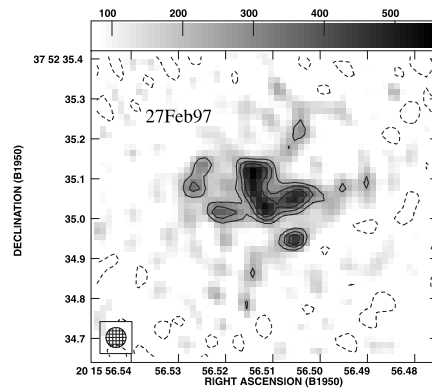
rms noise = 0.15 mJy/bm
peak flux = 1.18 mJy/bm



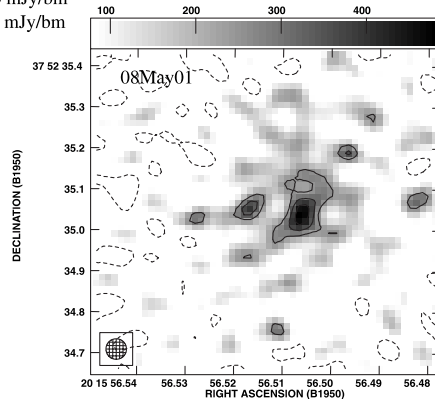
rms noise = 0.13 mJy/bm
peak flux = 0.81 mJy/bm



rms noise = 0.10 mJy/bm
peak flux = 1.00 mJy/bm



rms noise = 0.08 mJy/bm
peak flux = 0.58 mJy/bm



rms noise = 0.08 mJy/bm
peak flux = 0.51 mJy/bm

Table 2. The total flux densities (S_ν), the peak flux densities per beam and the corresponding peak brightness temperatures, T_b , for each epoch. For 1997 January 16 only a total value is given as because of poor signal-to-noise ratio the map is unreliable.

Date of observation	Total S_ν (mJy)	Peak S_ν (mJy beam $^{-1}$)	Peak T_b (10^3 beam $^{-1}$)
1992 July 1	8.4 ± 0.5	0.76 ± 0.11	7.4 ± 1.1
1992 August 4	11.3 ± 1.3	1.80 ± 0.23	17.5 ± 2.3
1997 January 15	8.9 ± 0.5	1.18 ± 0.15	11.5 ± 1.5
1997 January 16	10.4 ± 2.4	–	–
1997 January 19	9.4 ± 0.6	0.81 ± 0.13	8.0 ± 1.3
1997 January 30	5.8 ± 0.3	1.00 ± 0.10	10.0 ± 1.0
1997 February 27	6.4 ± 0.4	0.58 ± 0.08	5.7 ± 0.8
2001 May 8	4.8 ± 0.4	0.51 ± 0.08	5.0 ± 0.8

Table 3. The number, day, positions [RA(1950) $20^h 15^m 56^s+$, Dec. (1950) $37^\circ 52' 0''+$] and flux densities of the brightest peaks on the 1997 January maps. The position error is RA ≤ 0.006 s, Dec. ≤ 0.01 arcsec.

No.	date	RA	Dec.	Peak S_ν (mJy)
1	15	0.5145	35.07	1.18
2	15	0.5145	34.95	0.99
3	15	0.5081	35.01	0.72
4	19	0.5183	34.99	0.81
5	19	0.5107	35.01	0.77
6	19	0.5170	34.83	0.53
7	30	0.5119	35.04	1.00

To test the validity of the structures mapped, we decided to perform simulations. Data were created of an elliptical Gaussian point source of similar flux density to P Cygni and with various angular diameters, which had noise added to simulate real uv data. These were then mapped with precisely the same techniques as used on the P Cygni data sets. We found that to produce a map looking like the input data, the ratio of the maximum peak brightness to the rms (noise) should be ≥ 5 for the Gaussian source of angular diameter 50 mas, a value quite close to our peak-to-rms of 6 for most of our maps of P Cygni. For a larger angular diameter of 100 mas for the input model, the lower surface brightness means that a ratio of ≥ 7 is required before the map resembles the input model.

To improve the signal-to-noise ratio of our data we added together all of the data sets (the uv coverage is very similar for all data sets and position errors are much less than one beamsize, hence such a procedure is possible). If the source were intrinsically a single, unchanging ‘blob’, then such would be mapped from data of sufficient signal-to-noise ratio. However, the map produced from the sum of the six data sets from 1992 and 1997 shows instead a very inhomogeneous source, consisting of three main peaks of 10σ , 8σ and 6σ peak flux density (a similar result is obtained using only the 1997 data). Furthermore, alternative mapping of our data, using a weighting scheme that favours signal-to-noise ratio over resolution, produced maps essentially the same as those presented here, other than having lower resolution with peak-to-noise levels of 7σ to 11σ .

We therefore conclude that the mediocre signal-to-noise ratio of our data is not the cause of the inhomogeneous structures imaged, although we would add that only the brightest peaks on each map can be trusted. As a guide, of the peaks of Table 3, numbers 3 and 6

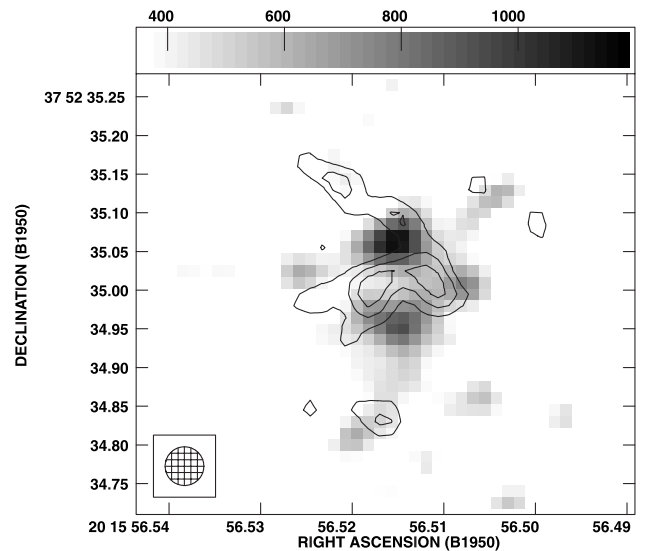


Figure 2. Two 1997 epochs of P Cygni shown on the same image. The grey-scale image is that of January 15 and the contour image is that of January 19. Contour levels go from 3σ to 5σ ($\sigma = 0.133$ mJy beam $^{-1}$). The grey-scale plot extends from 0.366 to 1.18 mJy beam $^{-1}$.

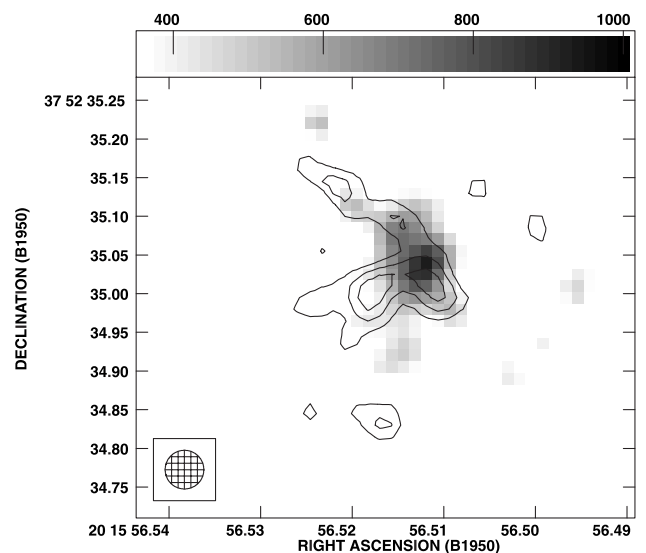


Figure 3. As for Fig. 2 but for January 19 (contours) and January 30 (grey-scale, scaled from 0.133 to 1 mJy beam $^{-1}$).

we do not believe are real. Although we are sure that the underlying structure of the radio-emitting material is blobby, we cannot be sure whether the imaged blobs are isolated structures or the brightest parts of larger structures, as at the signal-to-noise ratio levels of our data the two will look similar.

It is possible for interstellar scintillation (ISS) to cause variations over sufficient time-scales to make a single source look multiple and/or variable. P Cygni lies along the Galactic plane in a region of recent star formation, and so there is potentially enough material about to cause ISS. However, ISS affects only intrinsically very compact sources (see Rickett 1990). The largest limit at 6 cm is that for refractive ISS, for which it seems that source spatial scales of only a few mas are required for a significant effect – much larger will not show ISS – which is significantly less than the 50-mas resolution of our images. In addition, the time-scale over which refractive ISS has been suggested to occur is longer than the 16 h of

our observations, and thus it is unlikely to cause the clumpiness of our images (the time-scale of ISS is dependent on the source size and frequency). If ISS were affecting our observations, it would imply very compact structures of extremely high temperature (see Rickett 1986, 1990).

Finally, we should mention that it is possible that the variations occur over the duration of the observations, although this would indeed imply even smaller/clumpier/more unusual structure in the radio-emitting material. To obtain higher signal-to-noise ratio single-observation images of P Cygni, we must wait for the upgraded, e-MERLIN (<http://www.jb.man.ac.uk>).

5 DISCUSSION

5.1 The changing appearance of P Cygni

The appearance of P Cygni as imaged at 6 cm at a resolution of 50 mas is of a few peaks of emission of 0.5–1.2 mJy flux density within the inner 400 mas (note that 50 mas is 90 au or $250R_*$ for an 1800-kpc distance to P Cygni: Barlow & Cohen 1977; Lamers, de Groot & Cassatella 1983). The diameter of the 6-cm photosphere as estimated from fits to lower resolution (~ 0.35 arcsec) VLA data is 120 mas (White & Becker 1982), a value which increases to 195 mas if one updates the electron temperature T_e , to 10 000 K and the wind terminal velocity v_∞ to 206 km s^{-1} (Skinner et al. 1998). Since we detect no such large, unchanging photosphere, it is clear that the isothermal wind model as used by White & Becker is not valid, as was pointed out by Drew (1985). If what we see is the radio photosphere then it has a clumpy morphology.

The flux density measured from thermal free–free radiation from a wind, such as that from P Cygni (see e.g. Wright & Barlow 1975; Skinner et al. 1997), depends on both the electron temperature and the density. We can make a few simple calculations using the expression for the thermal free–free optical depth

$$\tau_{\text{ff}} = 8.24 \times 10^{-2} T_e^{-1.35} \nu^{-2.1} n_e^2 ds$$

(Osterbrock 1989), where ds is the distance over which the density, n_e , is integrated in pc, and ν is in GHz. Radio fluxes can be measured in terms of the brightness temperature, T_b , and for an isothermal nebula one has

$$T_b \rightarrow T_b \tau_{\text{ff}} \quad (\tau_{\text{ff}} \rightarrow 0),$$

$$T_b \rightarrow T_b \quad (\tau_{\text{ff}} \rightarrow \infty)$$

(Osterbrock 1989).

Using these equations, one can make some very simple calculations. According to Skinner et al. (1998), outside about $1000R_*$ (350 au) from the star the 6-cm emission from the wind should become optically thin (note that these regions are above where v_∞ has been reached), and in these regions T_e is about 11 000 K. Let us assume that our images resolve away the optically thin wind (MERLIN resolves out structure greater than ~ 800 mas) leaving only optically thick clumps; what values of n_e will be obtained from our data? Using the above equations for an optically thin wind (e.g. $\tau_{\text{ff}} = 0.1$) with T_e set to 10 000 K ($T_b = 1000$ K), we get $n_e = 7.3 \times 10^4 \text{ cm}^{-3}$, assuming $ds = 350$ au. For optically thick clumps ($\tau_{\text{ff}} = 1$) with $ds = 90$ au and also $T_e (= T_b) = 10 000$ K, we derive $n_e = 1.4 \times 10^5 \text{ cm}^{-3}$. These values are reasonably similar to the wind electron density of $2.8 \times 10^5 \text{ cm}^{-3}$ at $\sim 200R_*$ (Wright & Barlow 1975) calculated from the integrated light. If the clumps are smaller than 90 au then the T_b and calculated densities will increase. More reliable calculations of T_e

and n_e await data of higher resolution and better signal-to-noise ratio.

Over all the epochs observed, the morphology has changed, in one case over as little as 4 d (from 1997 January 15 to 19). Movement of material cannot occur fast enough to explain this, since to move a distance of even 10 au in 4 d would require a velocity of 4340 km s^{-1} – over 10 times the value of v_∞ . Although the brightest peaks in the January sequence of images (Figs 2 and 3) are not coincident, they do overlap between the three dates. A possible explanation for these variations may be changes to the ionization state of clumpy material. Recombination in high-density clumps could explain the rapid decrease in their radio emission. As suggested in Skinner et al. (1998), if the key cooling lines in the clumps are optically thick, their temperatures may be higher than the surrounding material. If these lines become optically thin because of expansion of the clump they will provide very efficient cooling, leading to a depopulation of the $n = 2$ level of hydrogen (from which photoionization maintains the ionization of the wind: Drew 1985), and with recombination of hydrogen the radio emission will disappear. The recombination time-scale for hydrogen atoms is $1.2 \times 10^5/n_e$ yr, so for a time-scale of 4 d, an electron density of 10^7 cm^{-3} within the clump is required; they would thus probably be smaller than 50 mas. Clumps disappearing in this manner would be replaced by new clumps that are also moving out in the wind; this allows the morphology to change more rapidly than simple movement of material would allow.

5.2 Is the wind of P Cygni clumpy?

From observations of the wind of P Cygni at other wavelengths, it is known to be inhomogeneous. Discrete absorption components appearing in the wind at $v < v_\infty$ in the optical and UV lines suggest the movement of shells through the wind (e.g. Markova 2000). Observed rapid spectropolarimetric variations are likely to be due to the wind being clumpy in the regions very close to the star, and simple modelling showed that the column density should vary by more than a factor of 10 to explain the degree of polarization variations detected (Taylor et al. 1991). Similar observations show clumps of ~ 0.1 –1 ster extent and density 10^{13} cm^{-3} (20 times ambient) very close to the stellar surface (Nordsieck et al. 2001). Optical interferometric observations by Vakili et al. (1997) detected a localized bright blob of moving gas, 0.8 mas ($4R_*$) to the south of the star. $H\alpha$ images of the regions further out in the wind were made by Chesneau et al. (2000) with an adaptive optics system. Their map showed the unresolved star to be surrounded by a clumpy envelope, with up to seven clumps of 50–100 mas diameter (close to the resolution limit), in the region 600 mas about the star, qualitatively very similar to our own results.

Observations of the extended nebula of P Cygni also show it to be clumpy or filamentary. Radio and optical images and spectra taken by Barlow et al. (1994), Skinner et al. (1998) and O’Connor, Meaburn & Bryce (1998) show that the nebula is inhomogeneous and quite extended (beyond 1 arcmin) and consists in the inner 20-arcsec region of dense neutral clumps being overtaken by the outflowing wind. The question to ask is what, if any, is the link between these outlying clumps and those detected closer in to the star (both below and above where v_∞ is reached)?

6 CONCLUSION

We have imaged the inner 400 mas of the outer wind of P Cygni with MERLIN at 6 cm. The maps, two from 1992, four from 1997

and one from 2001, show that the observed morphology changes, and that these changes can be quite rapid, as the sequence 1997 January 15–19–30 shows. Owing to the high resolution and accompanying low signal-to-noise ratio, we can only be sure that the brightest peaks on each date are real, and cannot be sure if they represent single structures or the brightest parts of larger structures. Since the wind and circumstellar environment of P Cygni is known to be clumpy, it seems reasonable to assume that the radio peaks represent emission from optically thick clumps, and the T_e and n_e derived from our data are consistent with the values determined by others, although we stress that our numbers should not be taken at face value as neither the true sizes of the structures nor the total flux density (as MERLIN resolves out larger-scale structure) is known. The rapid variations that we see are consistent with the rapid and random variations to the total flux density reported in Skinner et al. (1997). Recombination in cooling clumps, causing the radio flux to drop, and the appearance of other ionized clumps in the wind could result in such rapid morphological variations, but would require densities in the clumps of 10^7 cm^{-3} , 30 times the ambient value.

ACKNOWLEDGMENTS

MERLIN is a national facility operated by the University of Manchester on behalf of PPARC. SKW was supported by a Research Studentship Award from PPARC. We thank the controllers of MERLIN for the extra time awarded to observe P Cygni in 2001 May. We also thank the observers of the Carlsberg Automatic Meridian Telescope at La Palma.

REFERENCES

Baars J. W. M., Wendker H. J., 1987, *A&A*, 181, 210
 Baars J. W. M., Genzel R., Pauliny-Toth I. I. K., Witzel A., 1977, *A&A*, 61, 99

Barlow M. J., Cohen M., 1977, *ApJ*, 213, 737
 Barlow M. J., Drew J. E., Meaburn J., Massey R. M., 1994, *MNRAS*, 268, L29
 Chesneau O. et al., 2000, *A&AS*, 144, 523
 Drew J. E., 1985, *MNRAS*, 217, 867
 Duncan R. A., White S. M., Lim J., Nelson G. J., Drake S. A., Kundu M. R., 1995, *ApJ*, 441, 73
 Harries T. J., Hillier D. J., Howarth I. D., 1998, *MNRAS*, 296, 1072
 Israelian G., de Groot M., 1999, *Space Sci. Rev.*, 90, 493
 Krauss J. D., 1966, *Radio Astronomy*. McGraw Hill Book Co., London
 Lamers H. J. G. L. M., de Groot M., Cassatella A., 1983, *A&A*, 123, L8
 Markova N., 2000, *A&AS*, 144, 391
 Nordsieck K. et al., 2001, in de Groot M., Sterken C., eds, *ASP Conf. Ser. Vol. 233, IAU Workshop on P Cygni*. Astron. Soc. Pac., San Francisco, p. 261
 O'Connor J. A., Meaburn J., Bryce M., 1998, *MNRAS*, 300, 411
 Osterbrock D. E., 1989, *Astrophysics of Gaseous Nebulae and Active Galactic Nuclei*. University Science Books, Mill Valley, California
 Rickett B. J., 1986, *ApJ*, 307, 564
 Rickett B. J., 1990, *ARA&A*, 28, 561
 Scuderi S., Panagia N., Stanghellini C., Trigilio C., Umana G., 1998, *A&A*, 332, 251
 Skinner C. J., Exter K. M., Barlow M. J., Davis R. J., Bode M. F., 1997, *MNRAS*, 288, L7
 Skinner C. J., Becker R. H., White R. L., Exter K. M., Barlow M. J., Davis R. J., 1998, *MNRAS*, 296, 669
 Taylor M., Nordsieck K. H., Schulte-Ladbeck R. E., Bjorkman K. S., 1991, *AJ*, 102, 119
 Vakili F., Mourard D., Bonneau D., Morand F., Stee Ph., 1997, *A&A*, 323, 183
 Wendker H. J., Baars J. W. M., Altenhoff W. J., 1973, *Nature Phys. Sci.*, 245, 118
 White R. L., Becker R. H., 1982, *ApJ*, 262, 657
 Wright A. E., Barlow M. J., 1975, *MNRAS*, 170, 41

This paper has been typeset from a $\text{\TeX}/\text{\LaTeX}$ file prepared by the author.